Optica Applicata, Vol. LII, No. 4, 2022
DOI: 10.37190/oa220408

Optical trapping forces of focused circular partially coherent beams on Rayleigh particles

Chaoqun Yu[1], Fuchang Chen[1], Jun Zeng[1], Cheng Huang[1], Zhimin He[1], Huichuan Lin[1,*], Yongtao Zhang[1], Ziyang Chen[2], Jixiong Pu[1,2,**]

[1]College of Physics and Information Engineering, Minnan Normal University, Zhangzhou 363000, China

[2]Fujian Provincial Key Laboratory of Light Propagation and Transformation, College of Information Science & Engineering, Huaqiao University, Xiamen 361021, China

*Corresponding author: lhc1810@mnnu.edu.cn

**Corresponding author: jixiong@hqu.edu.cn

The optical trapping forces of tightly-focused radially polarized circular partially coherent beams on Rayleigh particles are theoretically investigated. Numerical calculations are performed to study the optical trapping forces on Rayleigh particles for different initial coherent length of the incident circular partially coherent beams. The results show that the magnitude of the gradient force decreases with the reduction of the initial coherent length of the focused radially polarized circular partially coherent beams, while the balanced position (*i.e.*, the position where the optical trapping forces becomes zero) stays constant. Moreover, the focused spot gradually elongates along the optical axis with the reduction of the initial coherent length, and the axial gradient force on Rayleigh particles also decreases gradually with the reduction of the intensity gradient in axial direction. As there exists an spherical aberrant in the focusing optical system, the focal spot in the direction of the optical axis becomes trumpet-shaped, and the optical trapping forces on Rayleigh particles change as well.

Keywords: tight focusing, radially polarized, circular partially coherent, spherical aberration, optical trapping force.

1. Introduction

Subwavelength focal patterns can be generated by focusing laser beams with a high numerical aperture (NA) objective [1–3]. With proper modulation on the phase and polarization of the incident beam, the patterns can be controlled, which have found applications in optical data storage, microscopy, particle beam trapping and material processing [4–11]. Extensive research efforts on tightly focused phase or polarization modulated beams have been carried out for decades [8]. The coherence property of light offers another degree for intensity modulation of tightly focused field. Previous

studies indicated that the spatial coherence of a partially coherent beam apparently influences the evolution behaviors of spectral density, degree of coherence, and state of the polarization [12–15].

On the other hand, significant advances have been achieved recently in designing and producing nonconventional correlation sources. Some novel partially coherent beams with peculiar correlation functions have been introduced, which exhibit nontrivial propagation properties such as far-field flat-topped, ring-shaped, self-focusing, self-splitting, optical cage and optical lattices [16–19]. For example, SANTARSIERO and his collaborators recently introduced the circular partially coherent light beams, which exhibits perfect coherence along any annulus but partial or even vanished coherence between two points with different radial distances [20,21]. DING *et al*. demonstrated the self-focusing property of such beam on propagation in oceanic turbulence [21]. LIN and his collaborators found that an optical needle with adjustable length along the optical axis can be obtained by regulating the coherent length of incident circular partially coherent beams [22,23]. Such non-diffracting optical needle may have potential applications in atom trapping, living biological cells manipulating, materials processing. To investigate the mechanical effect of circular partially coherent beams in a tightly focused scheme, the optical trapping forces of radially polarized circular partially coherent beams on Rayleigh particles are studied in this paper. In particular, since optical microscopes are commonly plagued by the aberrations, such as spherical aberration, defocus, and astigmatism *etc*. As an example, the effect of spherical aberration of the focusing system on the optical trapping force is also discussed.

2. Theoretical analysis

In this study, radially polarized circular partially coherent beams are employed as the incident laser beam, the cross-spectral density of the focal field formed by a high NA objective can be expressed as [23]

$$W_0(\mathbf{r}_1, \mathbf{r}_2) = \frac{I_0}{w_0^2}\exp\left(-\frac{r_1^2+r_2^2}{w_0^2}\right)\begin{bmatrix}\operatorname{sinc}\left(\dfrac{r_2^2-r_1^2}{\delta^2}\right)x_1x_2 & \operatorname{sinc}\left(\dfrac{r_2^2-r_1^2}{\delta^2}\right)x_1y_2\\ \operatorname{sinc}\left(\dfrac{r_2^2-r_1^2}{\delta^2}\right)y_1x_2 & \operatorname{sinc}\left(\dfrac{r_2^2-r_1^2}{\delta^2}\right)y_1y_2\end{bmatrix}$$

$$= \frac{E_0^2}{w_0^2}\exp\left(-\frac{r_1^2+r_2^2}{w_0^2}\right)\operatorname{sinc}\left(\frac{r_2^2-r_1^2}{\delta^2}\right)\begin{bmatrix}x_1x_2 & x_1y_2\\ y_1x_2 & y_1y_2\end{bmatrix} \tag{1}$$

In Eq. (1), $\operatorname{sinc}(x) = \sin(x)/x$, w_0 is the beam width, δ is the initial coherent length, $\mathbf{r} = (r, \varphi)$ is the position vector at the source plane, E_0 is the characteristic amplitude

of incident beam, and I_0 is the intensity of incident beam. It should be noted that the variables $\mathbf{r}_{1,2}$ in $W_0(\mathbf{r}_1, \mathbf{r}_2)$ are position vectors, while the other $r_{1,2}$ in Eq. (1) are scalars, because the cross-spectral density of radially polarized circular partially coherent beams is angle-independent. Additional, $r_{1,2}$ and $\psi_{1,2}$ are the magnitude and the angle in polar coordinates at the plane of incidence, respectively. $x_{1,2}$ and $y_{1,2}$ are the abscissa and the ordinate in Cartesian coordinates at the plane of incidence, respectively. Under the sine condition [24], *i.e.*, $r = f\sin\theta$, where f is the focal length of the objective, the two point pupil apodization correlation function of the incident beam can be expressed as [22]

$$\begin{aligned} F(\varphi_1, \varphi_2, \theta_1, \theta_2) &= \exp\left(-\frac{r_1^2 + r_2^2}{w_0^2}\right)\operatorname{sinc}\left(\frac{r_2^2 - r_1^2}{\delta^2}\right) \\ &= \exp\left[-\frac{f^2(\sin^2\theta_1 + \sin^2\theta_2)}{w_0^2}\right]\operatorname{sinc}\left[\frac{f^2(\sin^2\theta_2 - \sin^2\theta_1)}{\delta^2}\right] \end{aligned} \tag{2}$$

As the beam focused by a high NA objective, the second-order correlation properties of the focal field can be characterized by a 3×3 electric cross-spectral density matrix $W(\boldsymbol{\rho}_1, \boldsymbol{\rho}_2, \mathbf{z})$ [25]. In this study, after some tedious integration, the elements of the 3×3 matrix in the focal region can be obtained as follows:

$$\begin{aligned} W_{ij}(\rho_1, \rho_2, \psi_1, \psi_2, z) &= 4I_0\left(\frac{\pi}{\lambda}\right)^2 \int_0^\alpha \int_0^\alpha \frac{f^2}{w_0^2} \cos^{3/2}\theta_1 \cos^{3/2}\theta_2 \\ &\times \exp\left[-\frac{f^2(\sin^2\theta_1 + \sin^2\theta_2)}{w_0^2}\right]\operatorname{sinc}\left[\frac{f^2(\sin^2\theta_2 - \sin^2\theta_1)}{\delta^2}\right] \\ &\times \exp\left[ikz(\cos\theta_2 - \cos\theta_1)\right]\exp\left[-ik\beta f^4(\sin^4\theta_1 - \sin^4\theta_2)\right] \\ &\times M_{ij}(\rho_1, \rho_2, \psi_1, \psi_2, \theta_1, \theta_2)\,\mathrm{d}\theta_1\,\mathrm{d}\theta_2, \qquad (i, j = x, y, z) \end{aligned} \tag{3}$$

In Eq. (3), β is the spherical aberration coefficient, and $M_{ij}(\rho_1, \rho_2, \psi_1, \psi_2, \theta_1, \theta_2)$ for the elements on the primary diagonal of the $W(\boldsymbol{\rho}_1, \boldsymbol{\rho}_2, \mathbf{z})$ are

$$\begin{aligned} &M_{xx}(\rho_1, \rho_2, \psi_1, \psi_2, \theta_1, \theta_2) \\ &\quad = J_1(k\rho_1\sin\theta_1)J_1(k\rho_2\sin\theta_2)\sin^2\theta_1\sin^2\theta_2\cos\psi_1\cos\psi_2 \end{aligned} \tag{4}$$

$$\begin{aligned} &M_{yy}(\rho_1, \rho_2, \psi_1, \psi_2, \theta_1, \theta_2) \\ &\quad = J_1(k\rho_1\sin\theta_1)J_1(k\rho_2\sin\theta_2)\sin^2\theta_1\sin^2\theta_2\sin\psi_1\sin\psi_2 \end{aligned} \tag{5}$$

$$M_{zz}(\rho_1, \rho_2, \psi_1, \psi_2, \theta_1, \theta_2) = J_0(k\rho_1 \sin\theta_1) J_0(k\rho_2 \sin\theta_2) \sin^3\theta_1 \sin^3\theta_2 \sin\psi_1 \tag{6}$$

where J_0 and J_1 in Eqs. (4)–(6) are the zero-order and first-order Bessel functions of the first kind, respectively. By setting $\rho_1 = \rho_2 = \rho$ and $\psi_1 = \psi_2 = \psi$, the intensity of transverse polarized component of radially polarized circular partially coherent beams with negative spherical aberration in the focal region can be expressed as

$$I_{\text{transverse}}(\rho_1, \rho_1, \psi_1, \psi_1, z) = W_{xx}(\rho_1, \rho_1, \psi_1, \psi_1, z) + W_{yy}(\rho_1, \rho_1, \psi_1, \psi_1, z) \tag{7}$$

and the z-polarization component, *i.e.*, axial polarized light beams, is

$$I_z(\rho_1, \rho_1, \psi_1, \psi_1, z) = W_{zz}(\rho_1, \rho_1, \psi_1, \psi_1, z) \tag{8}$$

The total intensity distribution in the focal region is

$$I_{\text{total}}(\rho_1, \rho_1, \psi_1, \psi_1, z) = I_x(\rho_1, \rho_1, \psi_1, \psi_1, z) + I_y(\rho_1, \rho_1, \psi_1, \psi_1, z) + I_z(\rho_1, \rho_1, \psi_1, \psi_1, z) \tag{9}$$

In order to calculate the optical trapping force of radially polarized circular partially coherent beams with negative spherical aberration on nano- or micro-sized particles, for simplicity, it is assumed that the radius of the trapped particle is much smaller than the wavelength of the trapping laser, *i.e.*, the particle can be treated as a point dipole and Rayleigh scattering occurs. With this assumption, the gradient and scattering forces of the particle can be separated and expressed respectively as [26]

$$\mathbf{F}_{\text{g}}(\rho, z) = 2\pi a^3 \frac{n_2}{c} \frac{m^2 - 1}{m^2 + 2} \nabla I(\rho, z) \tag{10}$$

$$\mathbf{F}_{\text{s}}(\rho, z) = \frac{8}{3} \pi k^4 a^6 \frac{n_2}{c} \left(\frac{m^2 - 1}{m^2 + 2} \right)^2 I(\rho, z) \tag{11}$$

In Eqs. (10) and (11), a is the radius of the trapped particle, k is the wave-number, n_2 denotes the refractive index of the particle, n_1 denotes the refractive index of the ambient medium, $m = n_2/n_1$, and c is the speed of light in vacuum. Obviously, the gradient force $\mathbf{F}_{\text{g}}$ is proportional to the intensity gradient and points up the gradient when $n_2 > n_1$, and the scattering force $\mathbf{F}_{\text{s}}$ is proportional to the light intensity.

3. Results and discussions

For the focusing system without spherical aberration, *i.e.*, $\beta = 0$, the beam waists of the focused radially polarized circular partially coherent beams lie in the geometric

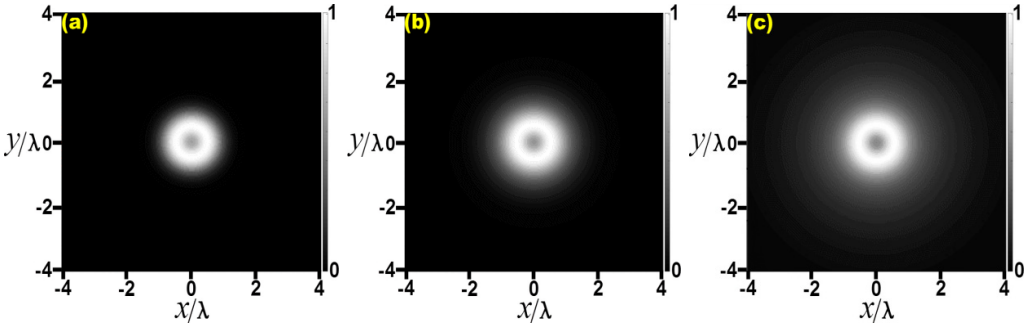

Fig. 1. Normalized intensity distribution of radially polarized circular partially coherent beams in the geometric focal plane of a high NA objective for different δ, (a) $\delta = w_0$, (b) $\delta = 0.6w_0$, and (c) $\delta = 0.2w_0$. The other calculation parameters are chosen as $\lambda = 633$ nm, $w_0 = 5$ mm, NA = 0.8, $f = 1$ cm, and $I_0 = 100$ mW/μm^2 and $\beta = 0$.

focal plane of the high NA objective. Figure 1 shows the total intensity distributions of radially polarized circular partially coherent beams in the geometric focal plane of a high NA objective for different initial coherent length. It could be concluded that although the spot size of the total intensity diffuses gradually with the decrease of initial coherent length, the lateral dimension of the dark hollow keeps nearly invariant. Because the gradient force of the focused light beams on Rayleigh particle is proportional to the intensity gradient, the diffusion of the intensity distribution means a decrease of radial gradient force. The invariance of the dark hollow of the intensity distribution probably means that the balanced position, where the gradient force is zero, does not change with coherent length.

Figure 2(a) shows the radial scattering force of the focused radially polarized circular partially coherent beams on the Rayleigh particle, which is assumed to be spherical and has a radius of 20 nanometers. Figure 2(b) indicates the radial gradient force

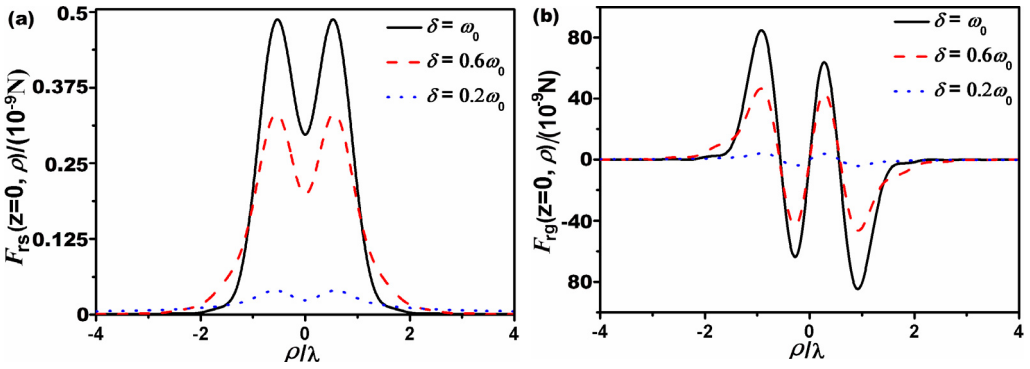

Fig. 2. The curve of radial scattering force and radial gradient force in focal plane for different initial coherent length, (a) radial scattering force, (b) radial gradient force. The other calculation parameters are chosen as $\lambda = 633$ nm, $w_0 = 5$ mm, NA = 0.8, $f = 1$ cm, $n_2 = 1.5$, $n_1 = 1.3$, $I_0 = 100$ mW/μm^2, $a = 20$ nm, and $\beta = 0$.

for different initial coherent length. A comparison between Fig. 2(a) and (b) demonstrates that both radial gradient force and radial scattering force reduce with the decrease of the initial coherent length, and the magnitude of radial scattering force is much smaller than the radial gradient force. Figure 2(b) shows that the balanced position, in geometric focal plane of the high NA objective, does stay constant as coherent length decreases.

Figure 3 presents the gradient force on Rayleigh particle which is represented by the red arrows, and the intensity distribution of the focused radially polarized circular partially coherent beams for different initial coherent length in ρ-z plane. Obviously, the intensity distribution of the focused radially polarized circular partially coherent beams in focal region gradually stretches along the optical axis as the initial coherent length decreases. Accompanied by the elongation of light spot in focal region along

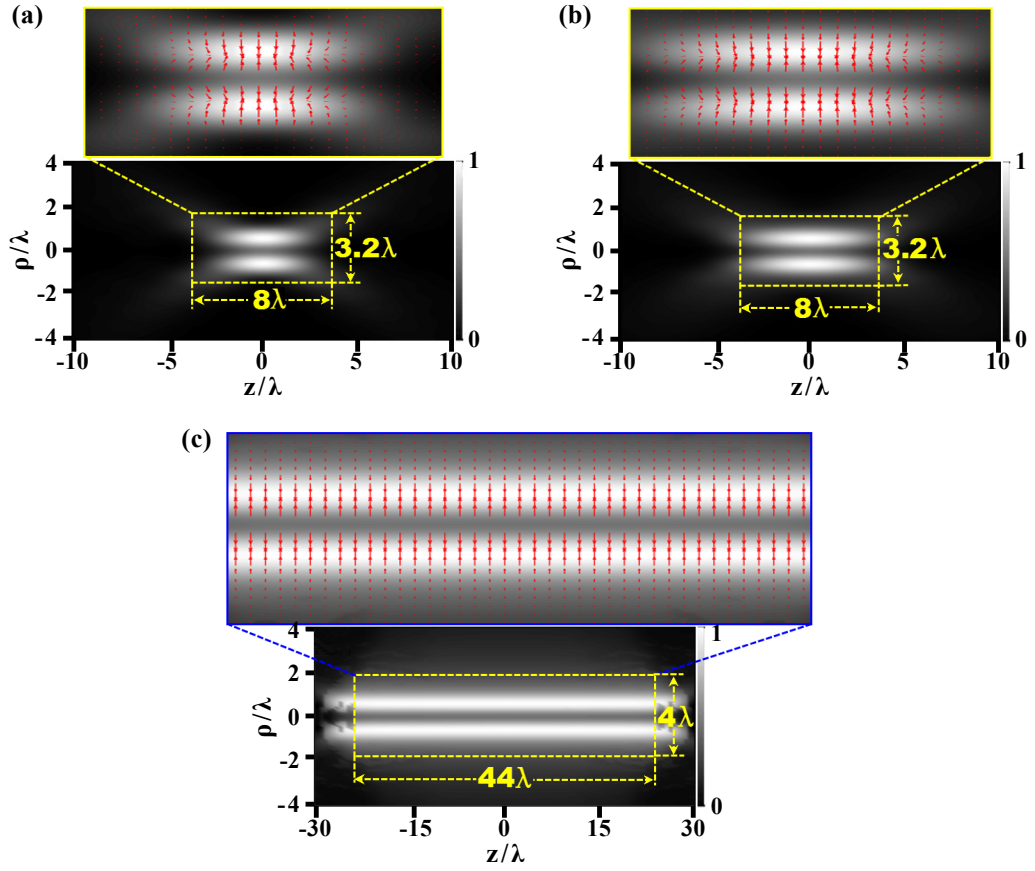

Fig. 3. Gradient force and intensity distribution in ρ-z plane of the focusing radially polarized circular partially coherent beams for different initial coherent length, (a) $\delta = w_0$, (b) $\delta = 0.6w_0$, and (c) $\delta = 0.2w_0$. Red arrows represent the direction of the gradient force, and the length of the arrows indicates the magnitude of the gradient force. The other calculation parameters are chosen as $\lambda = 633$ nm, $w_0 = 5$ mm, NA = 0.8, $f = 1$ cm, $n_1 = 1.3$, $n_2 = 1.5$, $I_0 = 100$ mW/μm^2, $a = 20$ nm, and $\beta = 0$.

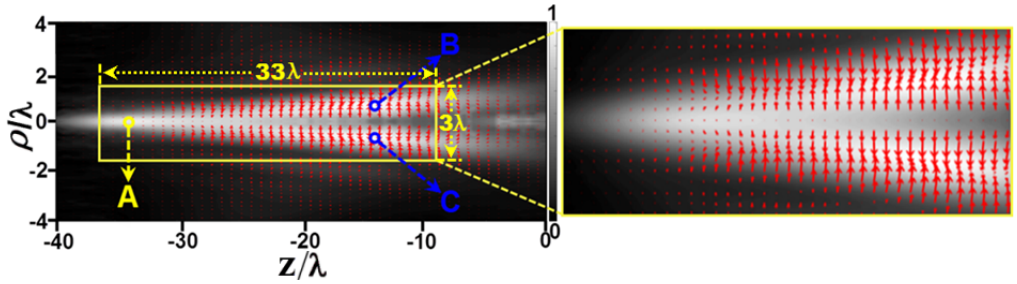

Fig. 4. Gradient force and intensity distribution of radially polarized circular partially coherent beams with negative spherical aberration in ρ-z plane near the focus. Red arrows represent the direction of the gradient force, and the length of the arrows indicates the magnitude of the gradient force. The calculation parameters are chosen as $\lambda = 633$ nm, $w_0 = 5$ mm, NA = 0.8, $\beta = 15 \times 10^{-4}$ mm^{-3}, $f = 1$ cm, $n_1 = 1.3$, $n_2 = 1.5$, $I_0 = 100$ mW/μm^2, $a = 20$ nm, and $\delta = 0.3w_0$.

the optical axis, the axial gradient force on Rayleigh particle, which is represented by the red arrows pointing along the optical axis, decreases gradually. As shown in Fig. 3(c), when the value of initial coherent length is $\delta = 0.2w_0$, the direction of the red arrows are all along the radius in the region of $-22\lambda \le z \le 22\lambda$, and $-2\lambda \le \rho \le 2\lambda$. It represents that when the value of initial coherent length is $\delta = 0.2w_0$, the axial gradient force can be regarded as zero in the region of $-22\lambda \le z \le 22\lambda$, and $-2\lambda \le \rho \le 2\lambda$.

The optical trapping force on nano- or micro-sized particles may be strongly influenced by the emerging aberrations. Thus, the effect of negative spherical aberration on the optical trapping force for Rayleigh particles is studied. When the spherical aberration of the focusing system is $\beta = 15 \times 10^{-4}$ mm^{-3}, the gradient force and intensity distribution of the focused radially polarized circular partially coherent beams in ρ-z plane near the focus are illustrated in Fig. 4. Apparently, when the focal system exists, the spherical aberration of the intensity distribution in ρ-z plane is stretched and becomes trumpet-shaped. In ρ-z plane, there are three peaks of light intensity, and they locate at $A(\rho = 0, z = -32\lambda)$, $B(\rho = 0.8\lambda, z = -13.6\lambda)$, and $C(\rho = 0.8\lambda, z = -13.6\lambda)$. The distribution of red arrows illustrates that these three points of the peak intensity are three balanced positions where the gradient forces are zero. Moreover, the axial gradient force is not equal to zero in the region of $-38\lambda \le z \le -5\lambda$, and $-1.5\lambda \le \rho \le 1.5\lambda$ as the spherical aberration of the focusing system is $\beta = 15 \times 10^{-4}$ mm^{-3}.

4. Conclusion

The optical trapping forces of tightly-focused radially polarized circular partially coherent beams on Rayleigh particles have been investigated theoretically through numerical calculations. The results demonstrate that the magnitude of the radial gradient force in focal plane decreases with the reduction of the initial coherent length of the focused radially polarized circular partially coherent beams, while the balanced position stays constant. The axial gradient force on Rayleigh particles also decreases gradually with the reduction of the initial coherent length. As there exists an spherical

aberrant in the focusing optical system, the focal spot in the axial direction becomes trumpet-shaped and the axial gradient force is no longer equal to zero.

Acknowledgements
This research was supported by the National Natural Science Foundation of China (NSFC) under grant numbers 61975072, 12174173, Natural Science Foundation of Fujian province under grant numbers 2022H0023, 2022J02047, 2022G02006, MSPY2022010, and the Natural Science Foundation of the Fujian Higher Education Institutions (JAT190393, 4202/B11967, KF2021103).

References

[1] HU K., CHEN Z., PU J., *Generation of super-length optical needle by focusing hybridly polarized vector beams through a dielectric interface*, Optics Letters **37**(16), 2012, pp. 3303–3305, DOI: 10.1364/OL.37.003303.
[2] LIU T., TAN J., LIU J., LIN J., *Creation of subwavelength light needle, equidistant multi-focus, and uniform light tunnel*, Journal of Modern Optics **60**(5), 2013, pp. 378–381, DOI: 10.1080/09500340.2013.778343.
[3] SUNDARAM C.M., PRABAKARAN K., ANBARASAN P.M., RAJESH K.B., MUSTHAFA A.M., *Creation of super long transversely polarized optical needle using azimuthally polarized multi Gaussian beam*, Chinese Physics Letters **33**(6), 2016, article no. 064203, DOI: 10.1088/0256-307X/33/6/064203.
[4] ZHAN Q., *Cylindrical vector beams: from mathematical concepts to applications*, Advances in Optics and Photonics **1**(1), 2009, pp. 1–57, DOI: 10.1364/AOP.1.000001.
[5] PING C., LIANG C., WANG F., CAI Y., *Radially polarized multi-Gaussian Schell-model beam and its tight focusing properties*, Optics Express **25**(26), 2017, pp. 32475–32490, DOI: 10.1364/OE.25.032475.
[6] PAYEUR S., FOURMAUX S., SCHMIDT B.E., MACLEAN J.P., TCHERVENKOV C., LÉGARÉ F., PICHÉ M., KIEFFER J.C., *Generation of a beam of fast electrons by tightly focusing a radially polarized ultrashort laser pulse*, Applied Physics Letters **101**(4), 2012, article no. 041105, DOI: 10.1063/1.4738998.
[7] PRABAKARAN K., SANGEETHA P., KARTHIK V., RAJESH K.B., MUSTHAFA A.M., *Tight focusing properties of phase modulated radially polarized Laguerre Bessel Gaussian beam*, Chinese Physics Letters **34**(5), 2017, article no. 054203, DOI: 10.1088/0256-307X/34/5/054203.
[8] ARBABI A., HORIE Y., BAGHERI M., FARAON A., *Dielectric metasurfaces for complete control of phase and polarization with subwavelength spatial resolution and high transmission*, Nature Nanotechnology **10**, 2015, pp. 937–943, DOI: 10.1038/nnano.2015.186.
[9] PFEIFFER C., GRBIC A., *Metamaterial Huygens' surfaces: Tailoring wave fronts with reflectionless sheets*, Physical Review Letters **110**(19), 2013, article 197401, DOI: 10.1103/PhysRevLett.110.197401.
[10] WANG J., *Advances in communications using optical vortices*, Photonics Research **4**(5), 2016, pp. B14–B28, DOI: 10.1364/PRJ.4.000B14.
[11] CHEN Z., HUA L., PU J., *Chapter 4 - Tight focusing of light beams: effect of polarization, phase, and coherence*, Progress in Optics **57**, 2012, pp. 219–260, DOI: 10.1016/B978-0-44-459422-8.00004-7.
[12] WOLF E., JAMES D.F.V., *Correlation-induced spectral changes*, Reports on Progress in Physics **59**(6), 1996, pp. 771–818, DOI: 10.1088/0034-4885/59/6/002.
[13] SETÄLÄ T., LINDFORS K., FRIBERG A.T., *Degree of polarization in 3D optical fields generated from a partially polarized plane wave*, Optics Letters **34**(21), 2009, pp. 3394–3396, DOI: 10.1364/OL.34.003394.
[14] ZHU S., WANG J., LIU X., CAI Y., LI Z., *Generation of arbitrary radially polarized array beams by manipulating correlation structure*, Applied Physics Letters **109**(16), 2016, article no. 161904, DOI: 10.1063/1.4965705.
[15] WANG J., HUANG H., CHEN Y., WANG H., ZHU S., LI Z., CAI Y., *Twisted partially coherent array sources and their transmission in anisotropic turbulence*, Optics Express **26**(20), 2018, pp. 25974–25988, DOI: 10.1364/OE.26.025974.

[16] KOROTKOVA O., *Random sources for rectangular far fields*, Optics Letters **39**(1), 2014, pp. 64–67, DOI: 10.1364/OL.39.000064.
[17] MA L., PONOMARENKO S.A., *Optical coherence gratings and lattices*, Optics Letters **39**(23), 2014, pp. 6656–6659, DOI: 10.1364/OL.39.006656.
[18] WAN L., ZHAO D., *Optical coherence grids and their propagation characteristics*, Optics Express **26**(2), 2018, pp. 2168–2180, DOI: 10.1364/OE.26.002168.
[19] SANTARSIERO M., MARTÍNEZ-HERRERO R., MALUENDA D., DE SANDE J.C.G., PIQUERO G., GORI F., *Partially coherent sources with circular coherence*, Optics Letters **42**(8), 2017, pp. 1512–1515, DOI: 10.1364/OL.42.001512.
[20] SANTARSIERO M., MARTÍNEZ-HERRERO R., MALUENDA D., DE SANDE J.C.G., PIQUERO G., GORI F., *Synthesis of circularly coherent sources*, Optics Letters **42**(20), 2017, pp. 4115–4118, DOI: 10.1364/OL.42.004115.
[21] DING C., KOIVUROVA M., TURUNEN J., PAN L., *Self-focusing of a partially coherent beam with circular coherence*, Journal of the Optical Society of America A **34**(8), 2017, pp. 1441–1447, DOI: 10.1364/JOSAA.34.001441.
[22] LIN H., ZHOU X., CHEN Z., SASAKI O., LI Y., PU J., *Tight focusing properties of a circular partially coherent Gaussian beam*, Journal of the Optical Society of America A **35**(12), 2018, pp. 1974–1980, DOI: 10.1364/JOSAA.35.001974.
[23] LIN H., LI Y., ZHOU X., WANG J., CHEN Z., PU J., *Generation of optical needle and dark channel by tight focusing of radially polarized circular partially coherent beams*, Optica Applicata **50**(2), 2020, pp. 229–240, DOI: 10.37190/oa200206.
[24] RICHARDS B., WOLF E., *Electromagnetic diffraction in optical systems. II. Structure of the image field in an aplanatic system*, Proceedings of the Royal Society of London. Series A, Mathematical and Physical Sciences **253**(1274), 1959, pp. 358–379.
[25] LINDFORS K., SETÄLÄ T., KAIVOLA M., FRIBERG A.T., *Degree of polarization in tightly focused optical fields*, Journal of the Optical Society of America A **22**(3), 2005, pp. 561–568, DOI: 10.1364/JOSAA.22.000561.
[26] LI D, WANG X, PU J., *The effect of astigmatism of focusing lens on potical trapping force*, Optical Technique **38**, 2012, pp. 268–272.

Received December 17, 2021
in revised form February 19, 2022